Chapter 17
Torsion Strength of Concrete Beams with Steel Fibers, Lightweight, or FRP: Data Driven Code Appraisal

Ahmed Awad, Jawad Ahmed, Ahmed F. Deifalla, Maged Tawfik, and Amr El-Said

Abstract Despite extensive research efforts directed toward the shear and torsional behavior of concrete elements, torsion strength remains an unexplored area. Numerous new materials are being used in construction as a result of advances in concrete technology. The use of lightweight concrete, steel-fiber reinforced concrete, and FRP-reinforced concrete are all kinds of advancements. The objective of the current work is to enhance torsion strength prediction for these three aspects. A summary of a series of power equation models for torsion strength based on a massive experimental database of 346 beams tested under torsion is outlined. The model validation is discussed. The developed models are accurate while remaining simple for design purposes.

Keywords Torsion · Lightweight concrete · FRP reinforced concrete · And Steel fibered concrete

A. Awad
Faculty of Engineering, October University for Modern Sciences and Arts, Giza, Egypt
e-mail: Amosad@msa.edu.eg

J. Ahmed
Swedish College of Engineering, Wah Cant, Pakistan
e-mail: Jawadcivil13@scetwah.edu.pk

A. F. Deifalla (✉)
Future University in Egypt, New Cairo, Egypt
e-mail: Ahmed.deifalla@fue.edu.eg

M. Tawfik
Department of Civil Engineering, The Higher Institute of Engineering, El Shrouk, Cairo, Egypt
e-mail: m.nashaat@sha.edu.eg

A. S. Mosallam et al. (eds.), *Advances in Smart Materials and Innovative Buildings Construction Systems*, Sustainable Civil Infrastructures,
https://doi.org/10.1007/978-3-031-47428-6_17

17.1 Introduction

A reliable design necessitates a thorough understanding of the characteristics of concrete components subjected to torsion (ACI-445 2013). Recently, the ACI examined torsion of all cases, including high-strength concrete (HSC), prestressed concrete (PC), and normal weight concrete (NWC) (ACI-445 2013). However, steel fiber reinforced concrete (SFRC), concrete with Fiber reinforced polymer (FRP), and lightweight concrete (LWC) were not discussed. Researchers all over the world are investigating the design and behavior of elements subjected to shear, torsion, and punching shear (ACI 213R-03 2014; Muttoni 2018; Kuchma et al. 2019; Deifalla et al. 2021; Deifalla 2020a, b, 2022, 2023; Badra and Deifalla 2022; Graybeal 2014; Greene and Graybeal 2013, 2015). Especially, torsion design and analysis of NWC beams require simplified, accurate, and unified approaches (Deifalla and Ghobarah 2014; Chalioris 2008; Chalioris and Karayannis 2009; Deifalla 2015; Deifalla et al. 2014; Deifalla et al. 2015; Hassan and Deifalla 2016; Rahal 2013; Deifalla 2020, 2021; ACI-318-19, ACI Committee 318 2019; prEC2: PT1prEN 1992-1-1/2018-04 2018). Although combined loading is the most common situation, most research studies have focused on pure torsion to distinguish the torsion effect (ACI-445 2013; Deifalla and Ghobarah 2014; Chalioris 2008; Chalioris and Karayannis 2009; Deifalla 2015; Deifalla et al. 2014; Deifalla et al. 2015; Hassan and Deifalla 2016; Rahal 2013; Deifalla 2021; Deifalla 2020c; ACI-318-19, ACI Committee 318 2019; prEC2: PT1prEN 1992-1-1/2018-04 2018). Very little guidance is offered by Design Codes and guides regarding the design of LWC, SFRC, and FRP reinforced beams (ACI 213R-03 2014; MC 2010; CSA 2004; EC2 2004; JSCE 2007; Nawaz et al. 2019; Khaloo and Sharifian 2005a).

For over two millenniums, the popularity of Lightweight concrete (LWC) in construction is growing (ACI 213R-03 2014). It has several advantages over NWC, including better insulation, and lower weight. On contrary, it had more cracking due to lower concrete stiffness. However, the experimentally observed behavior of LWC was found to be like that of the NWC (ACI 213R-03 2014). Recently, LWC is implemented in construction applications as it is considered a good alternative for NWC. These applications are as follows: (1) the walls whether curtain or structural; (2) marine structures or offshore; (3) folded plates and shell roofs; (4) bridge girders and decks; (5) beams and slabs that are precast, pre-tensioned, or post-tensioned; and (6) High-rise buildings elements walls, columns, and floors. LWC is helpful for the optimization of the reinforced concrete (RC) structures' construction process, self-weight, and member sizes (ACI 213R-03 2014). Using the LWC is better than NWC in achieving functional and architectural design (ACI 213R-03 2014). Thus, many extraordinary structures made of LWC are spread all around the world (ACI 213R-03 2014). The ACI Guides do not offer any recommendations for the torsion design of beams for LWC; instead, it directs practitioners to the ACI design codes, which are

primarily developed for NWC (ACI 213R-03 2014). Although LWC design guidelines are generally conservative, the design's consistency and economy are questionable. Since the economic factor governs the world directions towards all life aspects including RC structures.

With the economical aspect of design, thus, reducing safety factors, and improving the accuracy of the design models is the researcher's goal (ACI 213R-03 2014). Worldwide, FRP bars are noncorrosive; thus, used in many projects (ACI-445 2013; Muttoni 2018). The available design codes and guidelines, except the Canadian Standards Association (CSA), include detailed provisions only for shear and bending design of beams. While CSA includes torsion design. Thus, an objective for researchers is to provide practitioners with reliable design methods in torsion (Muttoni 2018). The design codes torsion provisions are lacking due to the following reasons: (1) shear and bending are more frequent compared to torsion; (2) if the applied torque is less than cracking torque, it can be neglected, and (3) Shear and bending are investigated much more than that for torsion. For the economy and safety of RC members. Since the complete comprehension of the torsion design is of the utmost importance, thus, it is still under investigation.

The design of FRP-RC beams under shear is attracting the core of research studies; thus, it is beneficial to examine the torsion behavior versus the shear behavior. Although shear and torsion strength in beams are formed by a set of diagonal and orthogonal internal forces, one of which is in compression and the other in tension, there are several distinctions between the two exist as follows: (1) Parallel pattern propagation for the shear cracks, while spiral pattern propagation for torsion cracks; thus, shear cracks spread in the same direction while torsion cracks spread in two opposite directions; (2) the torque strain varies in the three dimensions and it is non-uniform, while shear force strain varies in the two-dimension plane and it is uniform as well as perpendicular to the plane of applied shear; (3) mostly uniform stresses are developed due to shear forces, while in torsion cause bending on beam sides and thus the stress varies both horizontally and vertically across the cross-section. (4) the equivalent hollow tube thickness, which is resisting the applied torsion. In addition, it varies with the applied load. This is like the compression zone effective thickness in the case of bending moment; and (5) In flanged beams, the web mainly carries the shear forces, while the torque moments are carried by the flange and the web. The addition of steel fibers, which are available in various shapes and cross-sections, to the concrete mix leads to the creation of FRC. The characteristics are enhanced by the addition of steel fiber. Many researchers have extensively studied the behavior of this composite material. This current study aims at improving the torsion strength prediction for these three problems. A summary of a series of power equation models for torsion strength based on a massive experimental database of 346 beams tested under torsion is outlined. The model validation is discussed. Concluding remarks are outlined.

17.2 Model Development

17.2.1 Lightweight Concrete

Based on the existing previous investigations regarding the cracking torque, the following form is proposed as follows:

$$T_{cr} = c_1\left(\frac{1+0.004d}{2}\right)^{c_2}\left(\frac{3\gamma_c}{64}\right)^{c_3}F^{c_4}\left(f_c'\right)^{c_5}\left(\frac{A_c^2}{P_c}\right)^{c_6} \tag{17.1}$$

Thus, using the multi variable nonlinear regression using the gathered database, the following formula is proposed such that:

$$T_{cr} = 0.38\left(\frac{1+0.004d}{2}\right)^{-0.5}\left(\frac{3\gamma_c}{64}\right)^{1.07}F^{0.034}\left(f_c'\right)^{0.36}\left(\frac{A_c^2}{P_c}\right)^{1.14} \tag{17.2}$$

where d is the distance between the extreme compression fibers to the centroid of longitudinal tensile reinforcements (mm).

A_c is the total area of the concrete cross-section (mm^2).

p_c is the perimeter of the concrete section (mm).

γ_c is the unit weight of concrete (kN/m^3).

f_c' is the cylinder concrete compressive strength (MPa).

F is the fiber index.

17.2.2 Steel Fibered Concrete

Using multivariable nonlinear regression, the strength predictions of the strength of beams under torsion (T) for SFRC beams, can be such that:

$$T = \begin{cases} 0.19x^2y\sqrt{f_{cu}}(1+0.04F) & \textit{for rectagular cross section} \\ 0.1D^3\sqrt{f_{cu}}(1+0.08F) & \textit{for circular cross section} \\ 0.2\sum x^2y\sqrt{f_{cu}}(1+0.15F) & \textit{for flanged cross section} \end{cases} \tag{17.3}$$

While for SFRC beams, the torsional strength (T) can be such that:

$$T = 0.2\sum x^2y\sqrt{f_{cu}} + 0.13F\frac{x_oy_o}{x_o+y_o}xy\sqrt{f_{cu}} + kA_sf_{ty}\frac{x_1y_1}{s} \tag{17.4}$$

where x is the cross-smaller section's dimension.

x_0 is the smaller center-to-center dimension of the thin wall tube analogy, which is roughly equal to (5/6)x.

x_1 is the smaller dimension of the steel stirrup, which is taken approximately as 0.9 x.

y is the cross-bigger section's dimension.

y_0 is the bigger center-to-center dimension of the thin wall tube analogy, which is roughly equal to (5/6)y.

y_1 is the bigger dimension of the steel stirrup, which is roughly equal to 0.9 y.

A_s is the cross-sectional area of the stirrup.

f_{ty} is the yield strength of transverse reinforcement.

f_{cu} is the cubic compressive strength of the concrete.

F is the fiber index.

17.2.3 FRP Reinforced Concrete Beams

For torsion, Deifalla adapted the power-law equation, which was first proposed by Rahal with respect to the beams with Glass FRP. In addition, experimental investigations by Belarbi and Hsu were implemented. Thus, implementing the multi-variable non-linear regression, a model for the ultimate and cracking torsion was proposed. Thus, to capture nonuniform strain and stress distribution across the stirrups and the cross section (Deifalla 2022; Deifalla et al. 2015; Noshy et al. 2017). For cracking torque, all effective variables were included as follows: the concrete compression stress (f_c'), perimeter of cross section (p_c), area of cross section (A_c), such that:

$$T = \begin{cases} 0.19\left(A_c^2/p_c\right)^{0.9}\left(f_c'\right)^{1.15} \textit{ for rectangular cross section} \\ 0.09\left(A_c^2/p_c\right)^{0.9}\left(f_c'\right)^{1.15} \textit{ for rectangular cross section} \end{cases} \tag{17.5}$$

While for ultimate torsional moment, Nonlinear Multi-variable Regression was employed with the inclusion of all effective variables as follows: longitudinal reinforcement forces ($f_{Fu}A_l$), transversal reinforcement ratio $\left(\frac{f_yA_t}{s} + \frac{f_{Fu}A_t}{s}\right)$, cross section perimeter (p_c), the concrete compression stress (f_c'), and area of cross section A_c; such that:

$$T = 0.16(f_c\prime)^{0.67}A_c^{1.3}\left(\frac{f_yA_t}{s} + \frac{f_{fu}A_t}{s}\right)^{0.1}\left(f_{fu}A_l\right)^{0.12} \leq 0.34A_{oh}t_wf_c' \tag{17.6}$$

where A_{oh} is the enclosed area within the outermost closed stirrup's centerline (mm^2).

A_l is the torsion-resistant longitudinal reinforcement (mm^2).

A_t is the transversal reinforcement area that is bearing the torsion (mm^2).

s is the spacing between stirrups.

f_{fu} is the FRP bar's maximum tensile strength (MPa).

f_y is the yield strength of the longitudinal steel reinforcements (MPa).

t_w is the idealized hollow section's wall thickness, which is supposed to be no larger than the ratio of A_{oh}/ph or two times the minimum c (mm).

17.3 Model Validation

17.3.1 Lightweight

Table 17.1 shows the details and test results for the experimental LWC beams, while Table 17.2 and Fig. 17.1 show the ratio between the experimental torsional strength and that calculated using previous methods as well as the proposed model (PM1). For the cracking torque, the proposed model PM1 performance is more consistent and accurate but simple for design purposes compared to existing design codes. In addition, the coefficient of variation is 29% for the proposed model, while the existing model's coefficient of variation is 33%, 36%, and 29% for the ACI, CSA, and EC2, respectively. Moreover, the average values of the ratio between the measured torsional strength and that calculated using the ACI, the CSA, and the EC2, and the proposed model are 1.47, 1.32, 0.88, and 1.04, respectively. For the ultimate torque, the proposed model performance is more accurate and consistent but simple for design purposes compared to existing design codes. In addition, the proposed model coefficient of variation is 23%, while the existing model's coefficient of variation is 31%, 21%, and 25% for the ACI, CSA, and EC2, respectively. Moreover, the average values of the ratio between the measured strength and that calculated strength using the ACI, the CSA, and the EC2, and the proposed model are 1.30, 0.96, 1.00, and 1.21, respectively.

17.3.2 Steel Fibered Concrete

Table 17.3 shows the details and test results for the experimental steel-fibered concrete beams, while Table 17.4 and Fig. 17.2 show the ratio between the experimental torsional strength and that calculated using Nayraan and Karim model (NKPT) and the proposed models (PM2), and (PM3). The proposed model PM2 based on the Nayraan model is more accurate and consistent than the proposed model PM3 based on the ACI. The proposed model PM2 coefficient of variation is

Table 17.1 Details and test results for the experimental LWC beams database

#	ID	Cross section (mm)	Length (mm)	γc kN/m^3	f'_c MPa	f'_c MPa	T_{cr} kN m	T_u kN m
Nawaz et al. (2019)	LC-1–7	R200 × 100	700	15.45	6.97	1.21	0.71	0.71
	LC-1–14			15.45	7.17	1.21	0.72	0.72
	LC-1–42			15.35	8.18	1.31	0.75	0.75
	LC-1–90			15.27	8.38	1.31	0.77	0.77
	NC-2–7			16.46	12.22	1.62	0.87	0.87
	NC-2–14			16.51	15.25	1.72	0.97	0.97
	NC-2–21			16.36	16.67	1.82	1.00	1.00
	NC-2–42			16.31	18.69	1.92	1.03	1.03
	NC-3–7			15.96	11.62	1.52	0.85	0.85
	NC-3–42			15.66	17.78	1.92	1.02	1.02
	NC-4–21			15.15	14.75	1.72	0.96	0.96
	NC-4–42			15.20	16.67	1.82	0.99	0.99
	HC-5–7			18.18	48.58	3.13	1.65	1.65
	HC-5–14			18.08	50.00	3.23	1.67	1.67
	HC-5–21			18.13	55.95	3.33	1.85	1.85
	HC-5–42			18.08	59.09	3.43	1.79	1.79
	HC-6–14			18.08	57.17	3.43	1.91	1.91
	HC-6–21			18.03	60.60	3.54	1.84	1.84
	HC-6–28			18.08	66.36	3.64	2.09	2.09
	HC-7–3			19.19	27.67	2.42	1.49	1.49
	HC-7–7			19.24	42.52	2.93	1.58	1.58
	HC-7–21			19.19	58.58	3.43	1.92	1.92
	HC-7–42			19.17	66.46	3.74	2.09	2.09
	HC-8–7			17.13	21.21	2.12	1.26	1.26
	HC-8–14			17.07	26.56	2.32	1.28	1.28
	HC-8–42			17.07	36.66	2.73	1.49	1.49
	HC-9–7			20.72	52.82	3.33	1.74	1.74
	HC-9–14			20.63	68.28	3.74	1.92	1.92
	HC-9–28			20.63	78.28	4.04	2.29	2.29
	HC-10–7			20.36	48.58	3.13	1.72	1.72
	HC-10–28			20.30	74.44	3.94	2.16	2.16
	HC-10–42			20.30	82.21	4.14	2.16	2.16
Khaloo and Sharifian (2005a)	LC1	R200 × 100	700	17.85	9.09	1.41	0.73	0.73
	LC1-0.5–32			18.11	9.09	1.41	0.78	0.78
	LC1-1.0–32			18.37	9.09	1.41	0.81	0.81

(continued)

Table 17.1 (continued)

#	ID	Cross section (mm)	Length (mm)	γc kN/m^3	f'_c MPa	f'_c MPa	T_{cr} kN m	T_u kN m
	LC1-1.5–32			18.63	9.09	1.41	0.86	0.86
	LC1-2.0–32			18.90	9.09	1.41	0.92	0.92
	LC1-3.0–32			19.42	9.09	1.41	0.92	0.92
	LC2			19.20	12.12	1.62	0.88	0.88
	LC2-0.5–25			19.38	12.12	1.62	0.87	0.87
	LC2-0.5–32			19.38	12.12	1.62	0.91	0.91
	LC2-1.0–25			19.68	12.12	1.62	0.97	0.97
	LC2-1.0–32			19.68	12.12	1.62	1.01	1.01
	LC2-1.5–25			19.98	12.12	1.62	1.11	1.11
	LC2-1.5–32			19.98	12.12	1.62	1.17	1.17
	LC2-2.0–25			20.27	12.12	1.62	1.22	1.22
	LC2-2.0–32			20.27	12.12	1.62	1.30	1.30
	LC2-3.0–25			20.87	12.12	1.62	1.25	1.25
	LC2-3.0–32			20.87	12.12	1.62	1.33	1.33
	NC			17.60	30.30	2.53	1.44	1.44
	NC-0.5–32			17.77	30.30	2.53	1.48	1.48
Khaloo and Sharifian (2005b)	NC-1.0–32	R200 × 100	700	17.95	30.30	2.53	1.62	1.62
	NC-1.5–32			18.13	30.30	2.53	1.84	1.84
	NC-2.0–32			18.30	30.30	2.53	2.26	2.26
	NC-3.0–32			18.64	30.30	2.53	2.26	2.26
	HC			20.06	61.61	3.54	1.93	1.93
	HC-0.5–25			20.28	61.61	3.54	1.94	1.94
	HC-0.5–32			20.28	61.61	3.54	2.05	2.05
	HC-0.5–50			20.40	61.61	3.54	2.12	2.12
	HC-1.0–25			20.50	61.61	3.54	2.13	2.13
	HC-1.0–32			20.50	61.61	3.54	2.34	2.34
	HC-1.0–50			20.62	61.61	3.54	2.68	2.68
	HC-1.5–25			20.73	61.61	3.54	2.30	2.30
	HC-1.5–32			20.73	61.61	3.54	2.76	2.76
	HC-2.0–25			20.95	61.61	3.54	2.69	2.69
	HC-2.0–32			20.95	61.61	3.54	3.02	3.02
	HC-3.0–25			21.38	61.61	3.54	2.64	2.64
	HC-3.0–32			21.38	61.61	3.54	2.98	2.98
Yap et al. (2016)	OPSC-0	R100 × 100	500	18.48	34.24	3.33	0.00	0.00
	OPSC-25			18.91	39.69	4.34	0.22	0.23

(continued)

Table 17.1 (continued)

#	ID	Cross section (mm)	Length (mm)	γc kN/m^3	f'_c MPa	f'_c MPa	T_{cr} kN m	T_u kN m
	OPSC-50			19.33	41.61	5.45	0.25	0.26
	OPSC-75			19.78	46.36	6.77	0.29	0.30
	OPSC-100			20.22	47.77	8.28	0.29	0.31
	OPSC-0	R200 × 150	1500	19.90	33.13	2.83	5.54	5.56
	OPSFRC-55			20.89	34.74	3.64	7.35	7.43
	OPSFRC-65			20.61	35.86	3.94	7.85	7.96
	OPSFRC-80			20.91	37.37	3.94	8.67	8.69
Yap et al. (2015)	LR1	R300 × 150	2000	18.69	26.77	2.32	3.27	8.30
	LR2			18.69	29.29	2.42	4.36	9.27
	LR3			18.69	31.31	2.53	5.98	11.79
	LT1	T300 × 400/150 × 100		18.69	29.80	2.42	5.25	14.62
	LT2			18.69	30.81	2.53	8.36	18.82

Table 17.2 Model validation with respect to Lightweight concrete beams

	Statistical measure	ACI 19	CSA	EC2	PM1
Cracking torsion moment	Mean	1.47	1.32	0.88	1.04
	C.O.V (%)	33	36	29	29
Ultimate torsion moment	Mean	1.30	0.96	1.00	1.21
	C.O.V (%)	31	21	25	23

17%, while the existing model NKPT and the proposed model PM3 coefficient of variation are 22 and 19%. The average values of the ratio between the experimental torsional strength and that calculated strength using the existing NKPT model, and the proposed models PM2, and PM3 are 1.21, 1.01, and 1.02 respectively.

17.3.3 FRP Reinforced Concrete Beams

Table 17.5 shows the details and test results for the experimental FRP reinforced concrete beams, while Table 17.6 and Fig. 17.3 show the ratio between the experimental torsional strength and that calculated using the previous Hasan and Deifalla model (HD), the CSA, and the proposed model (PM4). For the cracking torque, the proposed model performance is more consistent and accurate but simple for design purposes compared to existing models. In addition, the coefficient of variation is 24% for the proposed model, while the existing model's coefficient of variation is

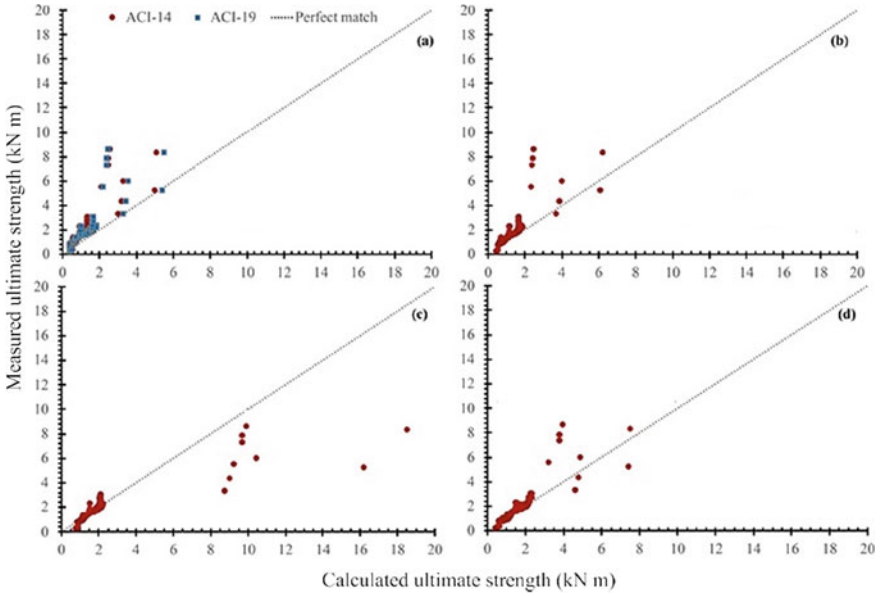

Fig. 17.1 The relation between experimental versus calculated ultimate torsional strength using: **a** the ACI, **b** CSA, **c** EC2, **d** PM1

63% and 37% for the CSA, and HD, respectively. Moreover, the average values of the ratio between the measured torsional strength and that calculated using the CSA, the HD model, and the proposed model PM4 are 1.33, 1.2, and 0.95, respectively. For the ultimate torque, the proposed model PM4 performance is more accurate and consistent but simple for design purposes compared to existing design codes. In addition, the proposed model coefficient of variation is 36%, while the existing model's coefficient of variation is 63% and 47% for the CSA, and HD, respectively. Moreover, the average values of the ratio between the measured torsional ultimate strength and that calculated using the CSA, the HD model, and the proposed model PM4 are 1.33, 1.65, and 1.24, respectively.

17.4 Conclusions

Three massive experimental databases of a total of 346 beams were tested under torsional moments. Four models were proposed for predicting the torsional strength of lightweight concrete beams, steel fiber reinforced concrete beams, and beams with FPR reinforcements, which is based on the database and using Multi-linear regression. The present work can reasonably lead to the following conclusions:

Table 17.3 Details and test results for the experimental steel-fibered concrete beams database

References	Cross section (mm)	ρ_f (%)	f_{cu} (MPa)	f_{ly} (MPa)	ρ_l (%)	f_{ty} (MPa)	ρ_t (%)	Tu (kNm)
Noshy et al. (2017)	R100 × 155	0.75	20.5	390	0.73	–	–	1.3
	R100 × 155	0.75	20.5	390	0.73	371	1.14	1.75
	R100 × 155	1.25	21.4	375	0.73	–	–	1.32
	R100 × 155	1.25	21.4	390	0.73	–	–	1.37
	R100 × 155	1.25	21.4	450	1.3	–	–	1.38
	R100 × 155	1.25	21.4	390	0.73	371	0.82	1.91
	R100 × 155	1.25	21.4	390	0.73	371	1.07	2.03
	R100 × 155	1.75	21.6	390	0.73	–	–	1.43
	R100 × 155	1.75	21.6	390	0.73	371	1.14	2.27
Sharma (1989)	R152 × 310	0.5	40.2	350	1.26	400	1.1	13.95
	R152 × 310	1	40.2	350	1.26	400	1.1	15.67
Kaushik and Sasturkar (1989)	R125 × 300	0.5	24.2	400	1.1	400	2.34	7.5
	R125 × 300	1	26.6	400	1.1	400	2.34	9
	R125 × 300	1.5	25.5	400	1.1	400	2.34	8.5
Al-Ausi et al. (1989)	R85 × 178	1.34	43.1	314	1.35	–	–	2.65
	R85 × 178	1.91	42.3	310	0.77	–	–	2.63
	R85 × 178	0.9	42.3	314	1.35	368	0.45	2.8
	R85 × 178	1.34	41.8	314	1.35	–	–	2.43
	R85 × 178	1.86	41.4	368	0.25	–	–	2.31
	R85 × 178	0.59	51.3	310	0.77	310	0.77	2.74
	R85 × 178	0.82	49.1	310	0.77	310	0.54	2.56
	R85 × 178	1.09	46.1	310	0.77	368	0.25	2.6
	R85 × 178	1.16	48.6	310	0.77	368	0.18	2.76
	R85 × 178	0.52	48.6	368	0.25	310	1.34	2.18
	R85 × 178	1.11	46.1	368	0.25	310	0.77	2.18
	R85 × 178	1.42	44.9	368	0.25	368	0.45	2.67
	R85 × 178	1.61	47.5	368	0.25	368	0.25	2.63
	R85 × 178	0.84	49.1	339	0.48	310	1.34	2.74
	R85 × 178	1.59	48.4	339	0.48	–	–	2.46
	R85 × 178	0.95	48.2	310	1.15	–	–	2.76
	R85 × 85	1.06	48.2	310	1.61	–	–	1.02
	R85 × 145	1.42	44.9	310	0.94	–	–	1.83
	R300 × 300	0.5	25.8	380	0.7	380	0.79	27.34
	R300 × 300	1	21.4	380	0.7	380	0.79	29.01

(continued)

Table 17.3 (continued)

References	Cross section (mm)	ρ_f (%)	f_{cu} (MPa)	f_{ly} (MPa)	ρ_l (%)	f_{ty} (MPa)	ρ_t (%)	Tu (kNm)
Narayanan and Kareem-Palanjian (1986)	R300 × 300	1.5	28	380	0.7	380	0.79	34.67
	R300 × 300	1	21.4	380	1.05	380	1.18	36.46
	R300 × 300	1	21.4	380	1.4	380	1.57	40.86
Mansur et al. (1989)	R100 × 200	0.6	31.2	250	1.57	250	0	1.41
	R100 × 200	1.2	40.1	250	1.57	250	0	1.74
	R100 × 200	0.6	38.9	250	1.57	250	0.35	2.29
	R100 × 200	1.2	35.6	250	1.57	250	0.35	2.84
	R100 × 200	0.3	40.1	500	1.01	500	1.68	5.56
El-Niema (1993)	R100 × 200	0.6	41.1	500	1.01	500	1.68	5.69
	R100 × 200	0.9	42	500	1.01	500	1.68	5.73
	R100 × 200	1.2	43.3	500	1.01	500	1.68	5.82
	R100 × 200	0.3	41.3	500	1.57	500	0.85	4.11
	R100 × 200	0.6	42.2	500	1.57	500	0.85	4.19
	R100 × 200	0.9	43.4	500	1.57	500	0.85	4.23
	R100 × 200	1.2	44.1	500	1.57	500	0.85	4.23
	R100 × 200	0.3	41.5	500	0.57	500	1.51	3.85
	R100 × 200	0.6	42.8	500	0.57	500	1.51	3.93
	R100 × 200	0.9	43.1	500	0.57	500	1.51	3.98
	R100 × 200	1.2	43.9	500	0.57	500	1.51	4.02
	R100 × 200	0.3	35.2	500	1.57	500	0.02	2.01
Rao and Rama Seshu (2005)	R100 × 200	0.6	37	500	1.57	500	0.02	2.27
	R100 × 200	0.9	37.7	500	1.57	500	0.02	2.61
	R100 × 200	1.2	38.4	500	1.57	500	0.02	2.82
	R100 × 200	0.3	33.9	500	0.14	500	2.51	1.75
	R100 × 200	0.6	34.4	500	0.14	500	2.51	2.31
	R100 × 200	0.9	35	500	0.14	500	2.51	2.57
	R100 × 200	1.2	35.3	500	0.14	500	2.51	2.69
Rao and Seshu (2006)	R100 × 200	1	17	415	1.57	–	–	2.41
	R100 × 200	3	16.4	415	1.57	–	–	2.73
	R100 × 200	1	19	415	1.57	344	0.75	2.73

(continued)

Table 17.3 (continued)

References	Cross section (mm)	ρ_f (%)	f_{cu} (MPa)	f_{ly} (MPa)	ρ_l (%)	f_{ty} (MPa)	ρ_t (%)	Tu (kNm)
	R100 × 200	3	16.9	415	1.57	344	0.75	3.15
Chalioris and Karayannis (2009b)	R100 × 200	0.3	51	432	1.57	432	1.51	6.67
	R100 × 200	0.6	51.8	432	1.57	432	1.51	6.76
	R100 × 200	0.9	52.5	432	1.57	432	1.51	6.84
	R100 × 200	1.2	53.9	432	1.57	432	1.51	6.93
	R100 × 200	0.3	51.1	432	1.57	432	0.8	5.22
	R100 × 200	0.6	52.1	432	1.57	432	0.8	5.3
	R100 × 200	0.9	53.4	432	1.57	432	0.8	5.39
	R100 × 200	1.2	54.1	432	1.57	432	0.8	5.47
	R100 × 200	0.3	52.6	432	0.57	432	1.51	5.77
	R100 × 200	0.6	53.2	432	0.57	432	1.51	5.82
	R100 × 200	0.9	54.1	432	0.57	432	1.51	5.9
	R100 × 200	1.2	55.5	432	0.57	432	1.51	5.99
Rao et al. (2010)	R150 × 200	0.3	33.4	460	0.67	460	0.55	4.58
	R150 × 200	0.6	31.3	460	0.67	460	0.55	5.68
	R150 × 200	0.3	31	460	0.67	460	0.55	4.94
	R150 × 200	0.6	30.9	460	0.67	460	0.55	5.87
	R150 × 200	0.3	32.7	460	0.67	460	0.55	4.92
	R150 × 200	0.6	29.5	460	0.67	460	0.55	5.88
	R150 × 200	0.3	31.9	460	0.67	460	0.55	4.85
	R150 × 200	0.6	30	460	0.67	460	0.55	5.49
	R150 × 200	0.3	31.7	460	1.51	460	0.55	6.01
	R150 × 200	0.3	31.6	460	1.51	460	0.55	6.25

Where $\boldsymbol{\rho_f}$ is the volume ratio of fibers
$\boldsymbol{\rho_l}$ is the longitudinal steel reinforcement ratio
$\boldsymbol{\rho_t}$ is the transversal steel reinforcement ratio
f_{ly} is The yield strength of longitudinal steel reinforcing bars
f_{ty} is The yield strength of transversal steel reinforcement

Table 17.4 Model validation with respect to steel fibered concrete beams

	Statistical measure	Existing model (NKPT)	PM2	PM3
Ultimate torsion moment	Mean	1.21	1.01	1.02
	C.O.V (%)	22	17	19

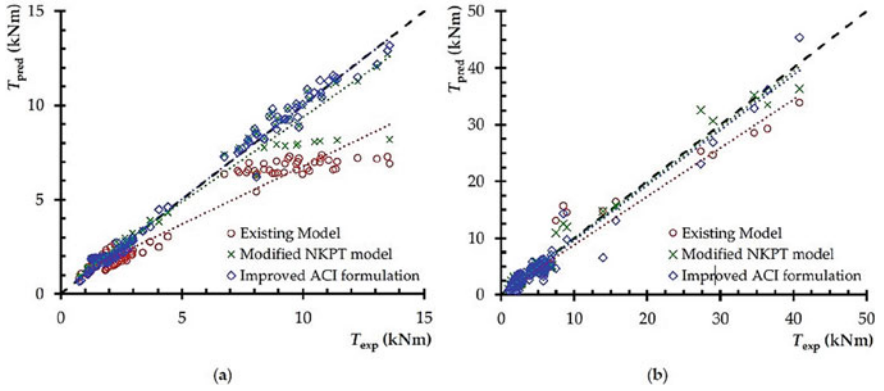

Fig. 17.2 Comparison of calculated and experimental ultimate torsion strengths for **a** L and T-beams and **b** R-beams

1. There is an absence of consensus among code provisions about many concepts, such as lightweight concrete, shear contribution for concrete, cracking torsional moment, size effect, angle of inclination of the strut, maximum nominal shear stress, and interaction between the torsion, shear, and moment.
2. The proposed model PM2 based on the NKPT model proved notably high efficiency in predicting torsional strength for steel fibered concrete beams and a lower coefficient of variation when compared to the NKPT model and the proposed model PM3 which is based on the ACI provisions.
3. The proposed model PM4 outperformed the previous Hasan and Deifalla model HD and the CSA provisions in predicting ultimate and cracking torsional strength for FRP-reinforced concrete beams.
4. The coefficient of variation and the average of the ratios between the experimentally measured torsional strength and that calculated showed that all the proposed models PM1, PM2, PM3, and PM4 are simple, consistent, and accurate, which are suitable for the purpose of design. These models could be the base for future design code developments.

Table 17.5 Details and test results for the experimental FRP beams database

References	Beam	f'_c MPa	*ffu* MPa	Dimensions (mm)	Conc. type	Long. Rfts	Trans. Rfts	T_{cr} (kN m)	T_u (kN m)
Okay and Engin (2012)	B5 B6	25 25	400 400	R200 × 100	NC NC	Steel (3φ10) and GFRP (2φ10) Steel (3φ10)	Steel 8 @ 200 mm Steel 8 @ 200 mm and GFRP 8 @ 200 mm	1.8 1.1	2.7 1.7
	B7	25	400		NC	Steel (3φ10) and GFRP (2 φ10)	Steel 8 @ 200 mm and GFRP 8 @ 200 mm	1.58	2.2
	B8	25	400		NC	GFRP (3φ10)	GFRP 8 @ 200 mm	0.86	1.2
	B9	25	400		NC	GFRP (3φ10)	GFRP 8 @ 200 mm	1.09	1.5
	B10	25	400		NC	GFRP (3φ10)	GFRP 8 @ 100 mm	0.58	1.1
	B11	25	400		NC	GFRP (2φ10)	GFRP 8 @ 100 mm	0.96	1.3
	B12	25	400		NC	GFRP (3φ10)	GFRP 8 @ 200 mm	1.14	1.6
	B13	25	400		NC	GFRP (3φ10)	GFRP 8 @ 200 mm	1.02	1.3
	B14	25	400		NC	GFRP (3φ10)	GFRP 8 @ 200 mm	1.31	1.8
	B15	25	400		NC	GFRP (3φ10)	GFRP 8 @ 200 mm	1.0	1.4
	B16	25	400		NC	GFRP (2φ10)	Steel 8 @ 100 mm	1.33	1.9
	B17	25	1500		NC	CFRP (3φ10)	Steel 8 @ 200 mm	1.91	1.9
	B18	25	1500		NC	CFRP (2φ10)	Steel 8 @ 200 mm	1.28	1.9

(continued)

Table 17.5 (continued)

References	Beam	f_c' MPa	*ffu* MPa	Dimensions (mm)	Conc. type	Long. Rfts	Trans. Rfts	T_{cr} (kN m)	T_u (kN m)
Shehab et al. (2009)	B1	30	360	R200 × 100	SCC	GFRP (4φ10)	GFRP 8 @ 100 mm	1.4	2.3
	B2	45	360		SCC	GFRP (4φ10)	GFRP 8 @ 100 mm	2.4	3.4
	B3	90	360		HSCC	GFRP (4φ10)	GFRP 8 @ 100 mm	3.0	4.5
	B4	45	360		SCSFC (0.75%)	GFRP (4φ10)	GFRP 8 @ 100 mm	3.0	3.8
	B5 B6	90 90	360 360		HSCSFC (0.75%) HSCSFC (1.5%)	GFRP (4φ10) GFRP (4φ10)	GFRP 8 @ 100 mm GFRP 8 @ 100 mm	3.0 4.0	5.0 5.1
Ragab and Eisa (2013)	BC120	38.5	1562	R600 × 250	NC	CFRP (8φ13)	CFRP 9.5 @ 120 mm	30.45	62.9
	BC180	38.5	1562		NC	CFRP (8φ13)	CFRP 9.5 @ 180 mm	29.87	49.4
	BC240	38.5	1562		NC	CFRP (8φ13)	CFRP 9.5 @ 240 mm	27.35	39.4
	BC300	38.5	1562		NC	CFRP (8φ13)	CFRP 9.5 @ 300 mm	28.65	35.7
Mohamed et al. (2015)	LB2	25	360	L350 × 150/150 × 400	NC	GFRP (2φ12)	Steel 6 @ 143 mm	2.1	8.4
	LB3	25	400		NC	GFRP (2φ12)	GFRP 6 @ 143 mm	2.1	10.0
	LB4	25	400		NC	GFRP (2φ12)	GFRP 8 @ 143 mm	2.1	14.0
	LB5	25	400		NC	GFRP (2φ12)	GFRP 10 @ 143 mm	2.1	20.0
Mohamed and Benmokrane (2015)	BG120	41.47	948	R600 × 250	NC	CFRP (7φ19)	GFRP 9.5 @ 120 mm	27.46	52.7
	BG180	41.47	948		NC	CFRP (7φ19)	GFRP 9.5 @ 180 mm	26.19	41.8

(continued)

Table 17.5 (continued)

References	Beam	f_c' MPa	*ffu* MPa	Dimensions (mm)	Conc. type	Long. Rfts	Trans. Rfts	T_{cr} (kN m)	T_u (kN m)
	BG240	38.5	948		NC	CFRP (7φ19)	GFRP 9.5 @ 240 mm	26.14	34.2
	BG300	41.47	948		NC	CFRP (7φ19)	GFRP 9.5 @ 300 mm	25.98	29.9
Mohamed and Benmokrane (2016)	BG-W	41.47	948	R600 × 250	NC	CFRP (8φ13)	–	23.11	25.0
	BG-120 BG-60	41.47 39.25	948 948		NC NC	CFRP (8φ13) CFRP (8φ13)	GFRP 9.5 @ 120 mm GFRP 9.5 @ 60 mm	27.46 27.76	52.7 56.9
	BC-W	38.5	1562		NC	CFRP (8φ13)	–	28.62	34.1
	BC120	38.5	1562		NC	CFRP (8φ13)	CFRP 9.5 @ 120 mm	30.45	62.9
	BC60	39.25	1562		NC	CFRP (8φ13)	CFRP 9.5 @ 60 mm	30.14	69.3
Zhou et al. (2017)	S-1	42.5	700	R150 × 200	PFC	GFRP (4φ14)	GFRP 8 @ 50 mm	2.88	5.5
	S-2	42.5	700		PFC	GFRP (8φ14)	GFRP 8 @ 50 mm	2.78	5.8
	F-1	40.2	700		PFC	GFRP (4φ14)	GFRP 8 @ 50 mm	2.88	6.7
	F-2	40.2	700		PFC	GFRP (8φ14)	GFRP 8 @ 50 mm	3.02	7.0
	F-3	40.2	700		CMC	GFRP (4φ14)	GFRP 8 @ 50 mm	2.78	5.7
	F-4	40.2	700		CMC	GFRP (8φ14)	GFRP 8 @ 50 mm	2.55	6.4
	E-1	32.8	700		CMC	GFRP (4φ14)	GFRP 8 @ 50 mm	2.28	8.2
	E-2	32.8	700		CMC	GFRP (8φ14)	GFRP 8 @ 50 mm	2.2	8.7

Table 17.6 Model validation with respect to FRP-reinforced concrete beams

	Statistical measure	CSA	HD	PM4
Cracking torsion moment	Mean	1.33	1.20	0.95
	C.O.V (%)	63	37	24
Ultimate torsion moment	Mean	1.33	1.65	1.24
	C.O.V (%)	63	47	36

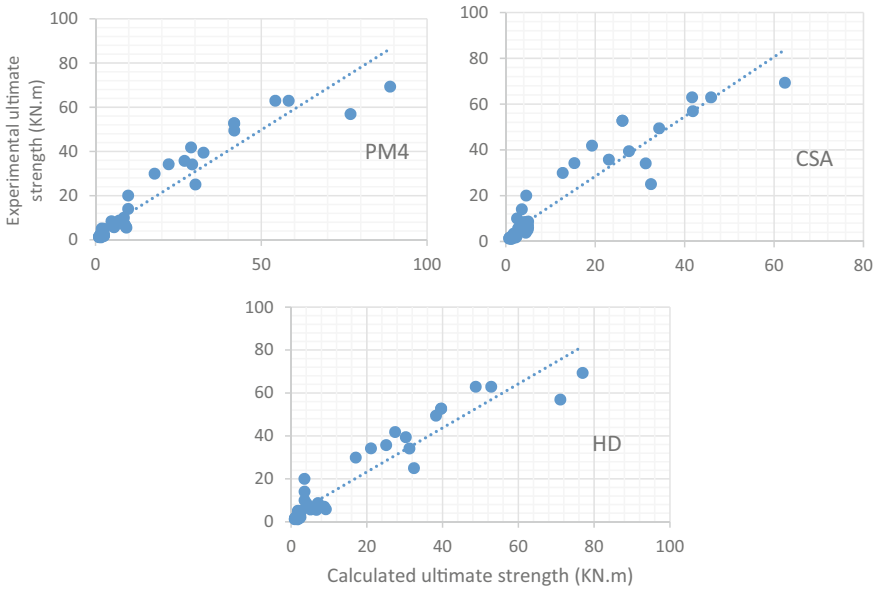

Fig. 17.3 The relation between experimental versus calculated ultimate torsional strength using PM4, CSA, and HD

References

ACI 213R-03 (2014) Guide for structural lightweight-aggregate concrete. ACI Committee 213. American Concrete Institute, Farmington Hills, Michigan, USA

ACI-318-19, ACI Committee 318 (2019) Building Code Requirements for Structural Concrete (ACI 318-19) and Commentary on Building Code Requirements (ACI 318-19). Farmington Hills (MI): American Concrete Institute

ACI-445 (2013) Report on torsion in structural concrete. Reported by Joint ACI-ASCE Committee 445. ACI 445.1R-12, ASCE-ACI Committee 445 on shear and torsion, April 2013, ISBN-13: 978-0-87031-810-8, ISBN: 0-87031-810-1, 80 pp

Al-Ausi MA, Abdul-Whab HMS, Khidair RM (1989) Effect of fibres on the strength of reinforced concrete beams under combined loading. In: Proceedings of the international conference held at the University of Wales, College of Cardiff, School of Engineering, Cardiff, UK, 18–20 September 1989; Elsevier Applied Science Publishers Limited; Elsevier Science Publishers: Essex, UK, pp 664–675

Badra N, Deifalla A (2022) Design reinforced concrete slabs with FRP reinforcements. In: Proceedings of the 7th international conference on civil structural and transportation engineering (ICCSTE'22) Niagara Falls, Canada–June 05–07, 2022, Paper No. 154. https://doi.org/10.11159/iccste22.154. Reliability-based evaluation of two-way shear.

Chalioris CE (2008) Torsional strengthening of rectangular and flanged beams using carbon fibre-reinforced-polymers-experimental study. Constr Build Mater 22(1):21–29

Chalioris CE, Karayannis CG (2009) Effectiveness of the use of steel fibers on the torsional behaviour of flanged concrete beams. Cem Concr Compos 31(5):331–341

CSA (2004) Design of concrete structures for buildings. Canadian Standards Association, Rexdale, Ontario, Canada

Deifalla A, Ghobarah A (2014) Behavior and analysis of inverted T-shaped RC beams under shear and torsion. Eng Struct 62:776–786

Deifalla A (2015) Torsional behavior of rectangular and flanged concrete beams with FRP reinforcements. J Struct Eng ASCE 04015068

Deifalla A (2020a) Design of lightweight concrete slabs under two-way shear without shear reinforcements: a comparative study and a new formula. Eng Struct Eng Struct 222:111076. https://doi.org/10.1016/j.engstruct.2020.111076

Deifalla A (2020b) Strength and ductility of lightweight reinforced concrete slabs under punching shear. Structures 27:2329–2345. https://doi.org/10.1016/j.is-truc.2020.08.002

Deifalla A (2020c) Torsion Design of lightweight concrete beams without or with fibers: a comparative study and a refined cracking torque formula. Structures 28:786–802. https://doi.org/10.1016/j.istruc.2020.09.004

Deifalla AF, Zapris AG, Chalioris CE (2021) Multivariable regression strength model for steel fiber-reinforced concrete beams under torsion. Materials 14:3889. https://doi.org/10.3390/ma14143889

Deifalla A (2021) Refining the torsion design of fibered concrete beams reinforced with FRP using multi-variable non-linear regression analysis for experimental results. Eng Struct 224

Deifalla A (2022) Data driven appraisal for one-way and two-way shear design of lightweight concrete and FRP-reinforced concrete elements. In: Proceedings of the 7th international conference on civil structural and transportation engineering (ICCSTE'22) Niagara Falls, Canada–June 05–07, 2022. Paper No. 203. https://doi.org/10.11159/iccste22.203.

Deifalla A (2023) Extended critical shear crack theory for punching shear of lightweight, FRP-reinforced, or prestressed concrete. In: Casini M (ed) Proceedings of the 2nd international civil engineering and architecture conference. CEAC 2022. Lecture notes in civil engineering, vol 279. Springer, Singapore. https://doi.org/10.1007/978-981-19-4293-8_37

Deifalla A, Hamed M, Saleh A, Ali T (2014) Exploring GFRP bars as reinforcement for rectangular and L-shaped beams subjected to significant torsion: an experimental study. Eng Struct 59:776–86

Deifalla A, Khalil MS, Abdelrahman A (2015) Simplified model for the torsional strength of concrete beams with GFRP stirrups. Compos Constr ASCE 19(1)

EC2 (2004) Eurocode 2: design of concrete structures–Part 1-1: general rules and rules for buildings. Incl. Corrigendum 1: EN 1992-1-1:2004/AC:2008, incl. Corrigendum 2: EN 1992-1-1:2004/AC:2010, incl. Amendment 1: EN 1992-1-1:2004/A1.: EN 1992-1-1:2004, 2014

El-Niema EI (1993) Fiber reinforced concrete beams under torsion. ACI Struct J 90.

Graybeal B (2014) Lightweight concrete: development of mild steel in tension. Technical Brief No. FHWA- HRT-14-030, Federal Highway Administration, Washington, DC

Greene G, Graybeal B (2013) Lightweight concrete: mechanical properties. Report No. FHWA-HRT-13-062, Federal Highway Administration, Washington, DC, 12 pp

Greene G, Graybeal B (2015) Lightweight concrete: shear performance," Report No. FHWA-HRT-15-022, Federal Highway Administration, Washington, DC, 20 pp

Hassan MM, Deifalla A (2016) Evaluating the new CAN/CSA-S806-12 torsion provisions for concrete beams with FRP reinforcements. Mater Struct. https://doi.org/10.1617/s11527-015-0680-9

JSCE (2007) Subcommittee on English version of standard specifications for concrete structures-2007 Japan Society of Civil Engineers (JSCE), December 2010, JSCE 2010 Concrete Committee, ISBN 978-4-8106-0752-9

Kaushik S, Sasturkar P (1989) Simply supported steel fibre reinforced concrete beams under combined torsion, bending and shear. In: Proceedings of the international conference held at the University of Wales, College of Cardiff, School of Engineering, Cardiff, UK, 18–20 September 1989; Elsevier Applied Science Publishers Limited; Elsevier Science Publishers: Essex, UK, pp 687–698

Khaloo AR, Sharifian M (Sep 2005a) Behavior of low to high-strength lightweight concrete under torsion. Int J Civ Eng 3(3&4):182–191

Khaloo AR, Sharifian M (2005b) Experimental investigation of low to high-strength steel fiber reinforced lightweight concrete under pure torsion. Asian J Civil Eng (Build Hous) 6(6)

Kuchma D, Wei S, Sanders D, Belarbi A, Novak L (Jul 2019) The development of the one-way shear design provisions of ACI 318-19. ACI Struct J 116(4). https://doi.org/10.14359/51716739

Mansur MA, Nagataki S, Lee SH, Oosumimoto Y (1989) Torsional response of reinforced fibrous concrete beams. ACI Struct J 86

MC (2010) Fédération internationale du béton. fib Model Code for Concrete Structures 2010. Lausanne; 2013

Mohamed HM, Benmokrane B (2016) Reinforced concrete beams with and without FRP Web reinforcement under pure torsion. J Bridge Eng 21(3):04015070. https://doi.org/10.1061/(ASCE)BE.1943-5592.0000839

Mohamed HM, Chaallal O, Benmokrane B (2015) Torsional moment capacity and failure mode mechanisms of concrete beams reinforced with carbon FRP bars and stirrups. J Compos Constr 19(2):04014049. https://doi.org/10.1061/(ASCE)CC.1943-5614.0000515

Mohamed HM, Benmokrane B (2015) Torsion behavior of concrete beams reinforced with GFRP bars and stirrups. ACI Struct J 112(5):543–552. https://doi.org/10.14359/51687824

Muttoni A (2018) Shear design and assessment: the coming steps forward for fib Model Code 2020. Struct Concr 19:3–4. https://doi.org/10.1002/suco.201870012

Narayanan R, Kareem-Palanjian AS (1986) Torsion in beams reinforced with bars and fibers. J Struct Eng 112:53–66

Nawaz W, Abdalla JA, Hawileh RA, Alajmani HS, Abuzayed IH, Ataya H et al (2019) Experimental study on the shear strength of reinforced concrete beams cast with Lava lightweight aggregates. Arch Civil Mech Eng 2019(19):981–996

Noshy A, Elwan S, Said H, Khalil A (Jan 2017) Torsional behavior of light weight concrete beams. Al-Azhar Univ Civ Eng Res Mag (CERM) 39(1)

Okay F, Engin S (2012) Torsional behavior of steel fiber reinforced concrete beams. Constr Build Mater 28:269–275

prEC2: PT1prEN 1992-1-1/2018-04 (2018) Eurocode 2: Design of Concrete Structures-Part 1-1: General rules for buildings, bridges and civil engineering structures. Third and final Draft by the Project Team SC2.T1

Ragab KS, Eisa AS (2013) Torsion behavior of steel fibered high strength self compacting concrete beams reinforced by GFRB bars. World Acad Sci Eng Technol Int J Civ Archit Sci Eng 7(9):331–341

Rahal K (2013) Torsional strength of normal and high strength reinforced concrete beams. Eng Struct 56:2206–2216

Rao TDG, Seshu DR (2006) Torsional response of fibrous reinforced concrete members: effect of single type of reinforcement. Constr Build Mater 20:187–192

Rao G, Seshu D, Warnitchai P (2010) Effect of steel fibers on the behavior of over-reinforced beams subjected to pure torsion. Civ Eng Dimens 12:44–51

Rao TDG, Rama Seshu D (2005) Analytical model for the torsional response of steel fiber reinforced concrete members under pure torsion. Cem Concr Compos 27:493–501

Sharma A (1989) Analysis of fiber reinforced concrete beams under combined loadings. Transp Res Rec 1226:94–104

Shehab HKHS, El-Awady M, Husain M, Mandour S (2009) Behavior of concrete beams reinforced by FRP bars under torsion. In: Proceedings of the 13th ICSGE, Cairo, Egypt, 6 pp

Yap SP, Khaw KR, Alengaram UJ, Jumaat MZ (2015) Effect of fibre aspect ratio on the torsional behavior of steel fiber-reinforced normal weight concrete and lightweight concrete. Eng Struct 2015(101):24–33

Yap SP, Alengaram UJ, Jumaat MZ, Khaw KR (2016) Torsional and cracking characteristics of steel fiber-reinforced oil palm shell lightweight concrete. J Compos Mater 50(1). https://doi.org/10.1177/0021998315571431

Zhou J, Shen W, Wang S (2017) Experimental study on torsional behavior of FRC and ECC beams reinforced with GFRP bars. Constr Build Mater 152:74–81